

Spectroscopy with a coherent dual frequency comb interferometer at 3.4 μm

Esther Baumann*, Fabrizio R. Giorgetta, Ian Coddington, William C. Swann,
and Nathan R. Newbury
NIST, 325 Broadway, Boulder, CO, USA 80305

ABSTRACT

A coherent dual fiber-comb spectrometer centered at 1.5 μm wavelengths is transferred to 3.4 μm by difference-frequency generation with a 1064 nm cw laser. It is shown that the residual linewidth between the comb teeth at 3.4 μm is resolution-limited to 200 mHz; such narrow linewidths can enable coherent dual-comb spectroscopy at high-precision and signal-to-noise ratio. We then discuss different interferometric configurations for coherent dual-comb spectroscopy. We find that a two-branch interferometric setup is appropriate to measure both the magnitude and phase spectrum of purely Doppler-broadened absorption lines. An initial measurement of methane lines in the ν_3 band P-branch with a resolution of 114 MHz is demonstrated.

Keywords: Frequency combs, Mid-IR, Molecular spectroscopy
Work of an agency of the US government, not subject to copyright

1. INTRODUCTION

Frequency combs have proven to be a powerful tool in a diverse range of applications, including broadband molecular spectroscopy [1-9]. However, standard frequency comb sources cover the visible to near-infrared portion (up to 2 μm) of the spectrum and do not extend out to longer mid-infrared (MIR) wavelengths, which are of interest for molecular spectroscopy because the fundamental absorption lines of many molecules are found in the 2 μm – 5 μm region.

Therefore, there have been a number of efforts to extend frequency combs to the MIR to support spectroscopic applications [3, 4, 10-12]. Here, we are interested in generating MIR frequency combs that can be used for fully coherent dual-comb spectroscopy since this method can provide both phase and magnitude spectra of a gas at high-precision and accuracy [7, 8]. Following established difference frequency generation (DFG) approaches [3, 4, 10-13], we generate MIR frequency combs through DFG in a periodically poled lithium niobate (PPLN) crystal between a cw 1064 nm fiber-laser source and two coherent Er-fiber-laser frequency combs at 1.5 μm . We then investigate different interferometric configurations to measure phase and magnitude spectra of purely Doppler-broadened ro-vibrational absorption lines of the C-H stretch in methane (CH_4).

2. COHERENT DUAL-COMB SPECTROSCOPY

2.1 Setup

A general setup for coherent dual-comb spectroscopy is shown schematically in Figure 1. This configuration was used in Ref. [8] to demonstrate high-precision and accuracy measurements of the ro-vibrational lines corresponding to the first C-H stretch in Hydrogen Cyanide (HCN) near 1550 nm. It makes use of a signal comb and a local oscillator (LO) comb with repetition frequencies $f_{r,S}$ and $f_{r,LO}$, respectively, that differ slightly by $\Delta f_r \equiv f_{r,S} - f_{r,LO}$. The combs are tightly phase locked together with less than a radian of optical phase noise (integrated from 1 Hz to the Nyquist frequency $f_r/2$), as described in the next section. The signal comb probes a sample under investigation and is then spatially superimposed with the LO comb. Detection of the added comb electric fields with a photodetector results in a multiheterodyne radio frequency (RF) comb, as seen in the left panel of Figure 2. The teeth spacing of the RF comb equals the difference in repetition rate of the signal and LO comb, Δf_r .

*esther.baumann@boulder.nist.gov; phone (303)497-3789, www.nist.gov

Provided that the comb spectral bandwidths are sufficiently narrow (as defined in the next paragraph), each RF comb tooth is related to the heterodyne beat between one specific pair of comb teeth from the transmitted signal comb and LO comb (see Figure 2 (a)). If the RF spectrum is scaled appropriately (by multiplying the frequency-axis by $f_r/\Delta f_r$ and applying an appropriate frequency offset), then the scaled RF spectrum is simply proportional to $H(\nu)E_S(\nu)E_{LO}^*(\nu)$, where $E_S(\nu)$ and $E_{LO}(\nu)$ are the comb electric field spectra, and $H(\nu)$ is the complex sample spectrum at optical frequencies, ν .

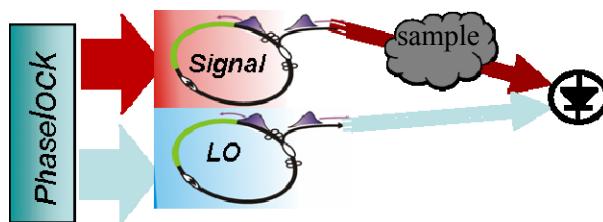


Figure 1: Schematic of dual-comb system. Two fiber frequency combs are tightly phase-locked together. The signal comb probes a gas sample, and is then combined with the LO comb on a detector. This results in a multiheterodyne RF comb with tooth spacing equal to the difference in repetition rate of signal and LO comb.

In a time-domain picture (Figure 2 (b)), the two combs produce a pulse train. Because of the difference in repetition rates, there is a pulse-by-pulse shift of $\Delta t = f_{r,LO}^{-1} - f_{r,S}^{-1} \approx \Delta f_r / f_r^2$ in the arrival time of the signal-pulses with respect to the LO-pulses. The overall relative time offset between the LO and signal-pulses ranges from 0 to $f_{r,S}^{-1}$ as the LO pulses walk through the signal pulses, and then repeats. If the detector signal is digitized synchronously with the LO pulse rate, then there are $N \equiv f_{r,LO} / \Delta f_r$ digitized samples acquired in a single update time $T_U \equiv \Delta f_r^{-1}$ as the LO pulse train completely walks through the signal pulse train. This single frame of data is simply the interferogram from the cross-correlation of the signal- and LO-pulses. Fourier transforming this dual-comb interferogram yields a spectrum that is equivalent to the RF comb discussed earlier, proportional to $H(\nu)E_S(\nu)E_{LO}^*(\nu)$, with a resolution of f_r and covering an optical bandwidth of $(2\Delta T)^{-1}$ about the carrier frequency of the signal- and LO-pulses. To generate spectra over broader bandwidths, one can scan the carrier frequency of the comb pulses using a tunable optical filter.

This interferogram is similar to the interferogram obtained in Fourier transform infrared spectroscopy (FTIR), where the light source is the signal comb and the moving mirror is replaced with the LO comb. Because the sample is placed in only the signal arm, the interferogram is analogous to a dispersive or asymmetric FTIR signal [14, 15] rather than a conventional FTIR signal where both beams pass through the sample. In the time-domain, the consequence of this geometry is that the sample interferogram is single-sided, with the free-induction decay of the excited molecules existing only after the excitation by the incident pulse. In the frequency-domain, the consequence is that both phase and amplitude of the sample are measured (similar to dispersive FTIR). We note that the combined speed and resolution of the dual-comb spectrometer would be challenging to achieve in a conventional FTIR spectrometer, as it would require a 1.5 m long mirror displacement at a speed of ~ 5 km/s to measure a spectrum with 100 MHz resolution in 300 μ s.

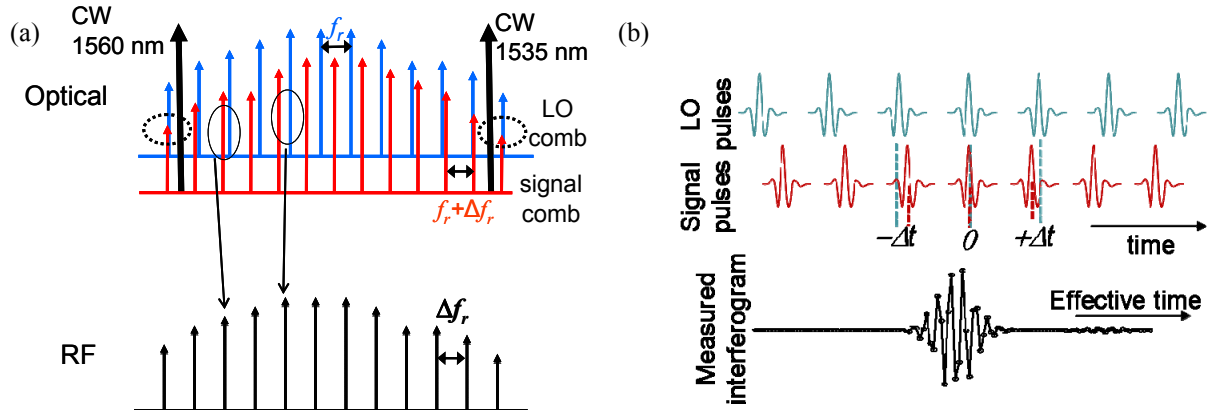


Figure 2: (a) Frequency-domain picture of coherent dual-comb spectroscopy illustrating the mapping of optical domain to RF domain. A signal comb with a repetition rate f_r is mixed with a LO comb (repetition rate $f_r + \Delta f_r$) on a detector, giving rise to a RF comb with tooth spacing Δf_r . (b) Time-domain picture (not to scale) of coherent dual-comb spectroscopy illustrating its analogy to Fourier spectroscopy. A single interferogram frame is measured as the pulses of the LO comb and signal comb walk through each other. The small wiggles to the right in the ‘measured interferogram’ are the result of free induction decay of a gas sample.

2.2 Phase-locking of the combs

Our dual-comb spectrometer relies on a tight mutual phase-lock of the signal and LO combs. The residual linewidth between both combs has to be much narrower than the difference in repetition rates, Δf_r , to achieve well defined comb teeth in the RF comb, as is evident in Figure 2(a). In fact, even narrower comb lines are required to allow for direct coherent signal averaging [8] since in this case the inverse linewidth sets the longest possible averaging time without needing to apply computationally intensive phase correction. To achieve these narrow relative comb lines, each comb is phase-locked to two cavity-stabilized cw fiber-lasers (at 1535 nm and 1560 nm), as was done in previous experiments [7, 8]. To lock the carrier frequency, the comb tooth adjacent to the 1560 nm laser is stabilized with a phase-locked loop that feeds back to both a high-bandwidth extra-cavity acousto-optic modulator to achieve ~ 0.5 rad phase noise and a low bandwidth intra-cavity piezo-electric transducer (PZT), which compensates for slow drifts. To fully phase stabilize the combs, their repetition rates have to be stabilized. Here, we phase-lock the comb tooth closest to the 1535 nm reference laser (see Figure 2 (a)) by feeding back to the current of the combs’ pump diodes.

By requiring both combs to have identical lock points separated by $\Delta \nu_{span}$ and choosing the smallest non-zero Δf_r by coarsely adjusting $f_{r,S}$ with an intracavity translation stage, we force the signal and LO combs to obey $f_{r,S} = \Delta \nu_{span} / N$ and $f_{r,LO} = \Delta \nu_{span} / (N + 1)$, where $\Delta \nu_{span}$ is the total frequency span between the two phase-locked teeth at 1560 nm and 1535 nm and the integer $N = f_{r,LO} / \Delta f_r$ is the frame length discussed above. Having an integer framelength N allows for straightforward time-averaging of subsequent frames to obtain a higher signal to noise ratio over a timescale given by the inverse of the residual linewidths. For even longer averaging times, the averaged interferogram frames can be phase-corrected before summing. For the setup of Ref. [8] and the data acquired here, $f_{r,S} \approx f_{r,LO} \approx 100$ MHz, $\Delta f_r = 3.14$ kHz, $\Delta t = f_{r,LO}^{-1} - f_{r,S}^{-1} \approx \Delta f_r / f_r^2 \approx 300$ fs, $T_U \equiv \Delta f_r^{-1} \approx 300$ μ s, $N \approx 32,000$, and $(2\Delta T)^{-1} \approx 1.6$ THz.

3. DUAL FREQUENCY COMBS AT 3.4 μ m WITH SUBHERTZ LINEWIDTHS

As already stated in the introduction, spectroscopy at wavelengths between 2 μ m and 5 μ m is important because of the strong fundamental absorption lines of many molecules. Here, we access the spectral region around 3.4 μ m by moving our fiber-laser based dual-comb system at 1.5 μ m via DFG to 3.4 μ m. In a first approach we used a fiber-

coupled ridge waveguide PPLN with a high conversion efficiency of 5 %/W [16]. Figure 3 shows the schematic of the setup. The outputs of the two coherent Er-fiber frequency combs (signal comb and LO comb) are combined, stretched by propagating through 700 m of SMF and amplified. The stretching of the pulse reduces nonlinearities in the amplifier and avoids pump depletion in the PPLN. The 1.5 μm light is then combined with the amplified 1064 nm cw fiber-laser light in a fiber coupler and directed to the fiber-coupled waveguide PPLN. The combined average comb power incident on the PPLN is ~ 2 mW, and the 1064 nm cw power is ~ 200 mW, resulting in a DFG comb power of ~ 20 μW . After the pump and signal light are removed with a germanium (Ge) window, the two 3.4 μm combs are detected on an InAs detector with a dark-current-limited noise equivalent power (NEP) of 15 pW/Hz^{1/2}.

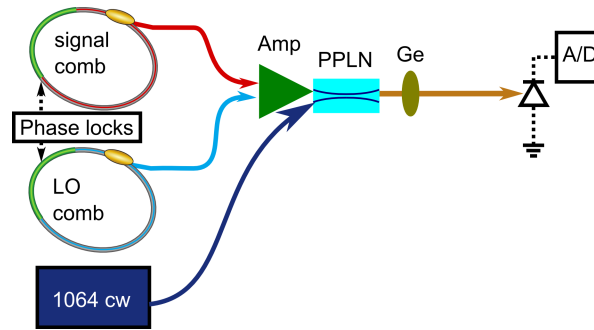


Figure 3: Schematic of 3.4 μm dual-comb setup. The two 1.5 μm combs are amplified and down-converted via DFG in a PPLN crystal with 1064 nm pump cw light. The light from the 1.5 μm combs and from the 1064 nm cw laser is filtered out by a Ge-window.

As illustrated in Figure 2(a), the RF spectrum of the detected signal yields an RF comb; the linewidth of the RF-comb teeth will reflect the residual linewidth between the signal comb and the LO comb. Figure 4 shows the heterodyne beats for the quasi-phase-matching condition centered at 1556 nm. We clearly observe the individual RF beats between pairs of comb teeth. The RF frequency f is linked to the optical wavelength λ by $\lambda = c / \{ \nu_{1064} - (\nu_{1560} + Nf) \}$, where c is the vacuum speed of light, ν_{1064} is the frequency of the 1064 nm laser, and ν is the frequency of the comb tooth locked to the 1560 nm cw reference laser. For these data, the wavelength, λ , spans 3.37 μm to 3.38 μm , and is given as the top axis of Figure 4. This conversion wavelength window is set by the quasi-phase-matching condition of the PPLN and can be shifted by tuning the PPLN temperature.

As expected, the residual linewidths of the beat notes between the combs are conserved through the DFG. For the full five seconds of data acquisition (limited by the on-board memory of the digitizer), we find a resolution-limited residual linewidth of 200 mHz, as seen in Figure 4 (c). Therefore, the absolute linewidth of the 3.4 μm comb will be limited by the absolute linewidth of the 1064 nm pump laser, which is ~ 1 MHz for our free running 1064 nm cw laser and could be reduced to hertz levels by locking it to a stable optical reference.

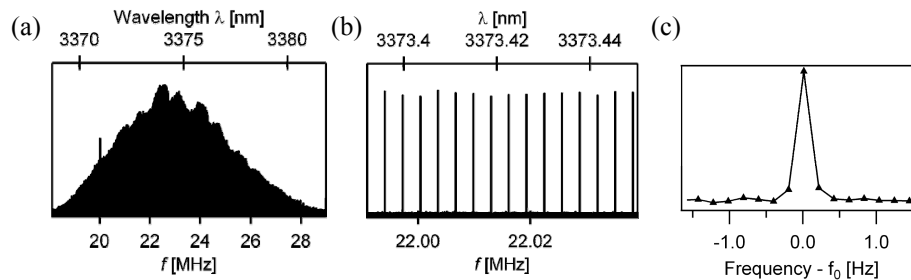


Figure 4: (a) Multiheterodyne comb measured at 3.4 μm ; the irregular spectral shape is caused by etaloning in the ridge waveguide PPLN and the Ge filter window. (b) Expanded view around 22 MHz showing the individual comb teeth. (c) Expanded view of a single comb tooth showing the residual linewidth of 200 mHz, limited by the five seconds observation period.

4. INTERFEROMETRIC DUAL-COMB CONFIGURATION FOR SPECTROSCOPY AT 3.4 μm

If the relatively simple configuration shown in Figure 3 is used for spectroscopy, only the magnitude of spectral features is obtained as both the signal and LO-pulses are co-propagating. In addition, the nonlinear cross-talk between LO and signal comb pulses co-propagating in the fiber amplifier leads to pulse distortion; this results in a highly featured baseline which introduces significant errors in the frequency calibration of the spectrum. Hence we investigated two different interferometric setups which avoid the pulse-to-pulse distortions and measure both phase and magnitude, as in dispersive or asymmetric FTIR, but at the cost of a more complex setup.

4.1 Single-branch interferometric configuration with one PPLN

Figure 5 shows the schematic of the single-branch interferometric setup. It is the same setup as discussed in the previous section, except that after the waveguide PPLN, the collimated 3.4 μm light is split into a measurement path (where a gas cell can be placed) and a time delayed reference path. Just before the detector, both paths are again overlaid and focused on the InAs diode.

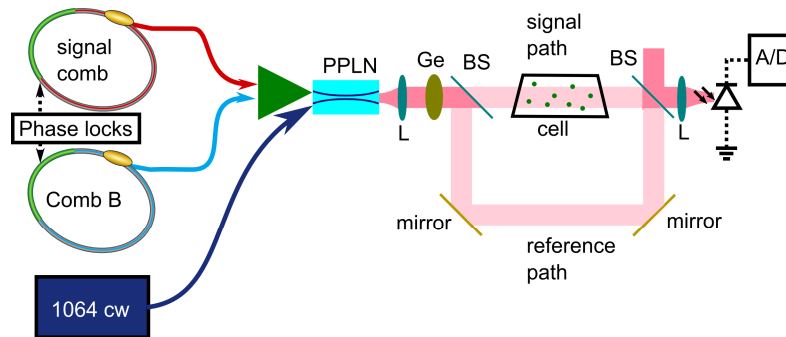


Figure 5: Schematic of the single-branch interferometric setup with one PPLN. All the lenses (L) and beamsplitters (BS) are CaF_2 . The Ge-window filters the 3.4 μm light from the pump and the signal.

In the time-domain, three distinct interferograms are detected, as seen in Figure 6. The center double-sided interferogram is generated from the signal- and LO-pulses co-propagating in the reference path or the measurement path and suffers from the pulse distortion discussed above (only one center interferogram is visible, as the delay between both interferograms is chosen to be $\sim f_r^{-1} / 4 = 2.5$ ns, which is smaller than the 10 ns sampling period of the digitizer). The satellite interferograms are generated from the delayed LO-pulse from the reference path probing the signal-pulse from the measurement path (and vice versa). As the two contributing pulses from the measurement and reference paths do not interact in the fiber amplifier (because they do not overlap in time), they do not suffer from pulse distortions.

As only one pulse is probing the sample in the satellite interferograms, they are single-sided and therefore contain both phase and amplitude information. As both satellite interferograms contain the same information, they are individually apodized, Fourier transformed, and co-added. Due to the splitting of one temporal frame into two single-sided and one double-sided interferograms (see also Figure 6 (a)), the required apodization is about one quarter of the total frame and therefore limits the frequency resolution to about four times the combs' repetition rate (in our case 400 MHz), which makes this configuration not well suited to measure most purely Doppler-broadened molecular lines that have sub-gigahertz linewidths. The right panel of Figure 6 shows a zoom in on the center part of the three interferograms while some purely Doppler-broadened methane lines around 3.4 μm are being measured. Those lines are narrower than the 400 MHz resolution provided by the setup, and one clearly sees that the individual interferograms overlap. It is then impossible to isolate the desired satellite interferogram.

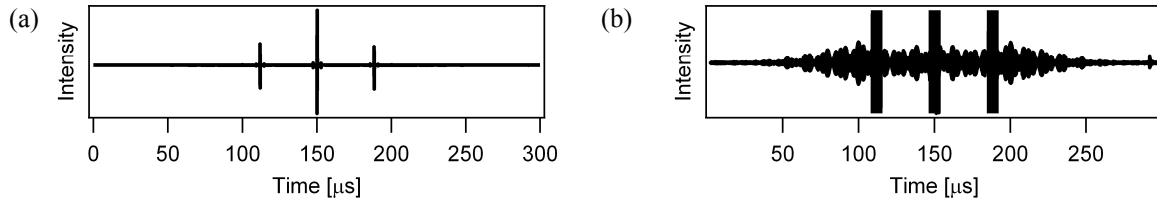


Figure 6: Time-domain interferograms of the single-branch interferometric setup. (a) Three distinct interferograms are seen in one frame; a double-sided center interferogram, and two single-sided satellite interferograms. (b) Expanded view of the interferograms with sub-Torr pressure methane gas in the cell. The methane absorption lines are purely Doppler-broadened and therefore give rise to a long signal in the time-domain. The signals from the three interferograms then overlap, and it is then impossible to isolate the desired satellite interferograms for such a narrow spectral line.

4.2 Two-branch interferometric setup

To avoid this overlap problem, we constructed another interferometer, similar in principle to Figure 1 and shown schematically in Figure 7, where the light from each comb is combined with the 1064 nm light in two separate branches. This configuration generates one single-sided sample interferogram without pulse-to-pulse distortions, which allows for a measurement of both phase and magnitude at the maximal resolution equal to the comb repetition rate (100 MHz). This gain in resolution, however, comes at the cost of doubling the PPLNs and the amplifiers for both combs and the 1064 nm cw light.

We use two bulk 10 mm long PPLNs in this configuration. The combs are filtered with a ~ 6 nm FWHM optical bandpass filter, which is close to the phase-matching bandwidth provided by the 10 mm long PPLN. This bandwidth is also a reasonably large fraction of the maximum allowed instantaneous measurement bandwidth of $(2\Delta T)^{-1} \approx 1.6$ THz (~ 12.5 nm at $1.5 \mu\text{m}$) while still suppressing aliasing. The 1064 nm light power at each PPLN is ~ 300 mW, and the filtered, amplified comb power is ~ 200 mW in each branch. The 1064 nm pump light and the comb light are superimposed with a fiber combiner and focused into the crystal with an aspheric lens of 18.4-mm focal length. A conversion efficiency of $\sim 10^{-4}$ / W is achieved, resulting in $\sim 10 \mu\text{W}$ of $3.4 \mu\text{m}$ light in each branch. The $3.4 \mu\text{m}$ signal comb passes through the measurement branch (and thus the gas cell) and is then combined with the unperturbed $3.4 \mu\text{m}$ LO comb. After again removing 1550 nm signal and 1064 nm pump light with a Ge-wedge, detection of the superimposed $3.4 \mu\text{m}$ combs with the InAs results in a single-sided interferogram. By using both the wedged bulk PPLNs and a Ge-wedge, most of the etaloning observed in Figure 4 was removed.

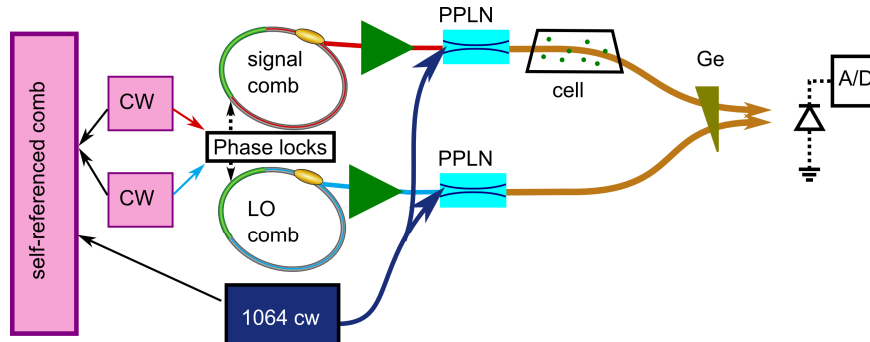


Figure 7: Dual-branch interferometric setup. The LO and signal combs are separately down-converted in a PPLN with a portion of the 1064 nm pump. The $3.4 \mu\text{m}$ combs are combined only after the gas cell in a CaF_2 beamsplitter (not shown in the schematic) and then focused on the detector. The 1560 nm and 1535 nm cw cavity-stabilized lasers used for the phase-locks of the signal and LO combs are referenced to a self-referenced comb. This self-referenced comb is also used to track the frequency of the 1064 nm pump during the measurement.

To obtain absolute frequency accuracy of ~ 1 MHz, a small portion of the 1064 nm light is counted with a self-referenced comb during the measurement (the same comb was used to determine the absolute frequencies of the cavity-stabilized 1560 nm and 1535 nm cw lasers to which the LO and signal combs are phase-locked). The accuracy is limited

by the free-running 1064 nm light to 1 MHz. The slowly varying baseline is removed by fitting a 10th-order polynomial to the spectra after masking the molecular absorption features.

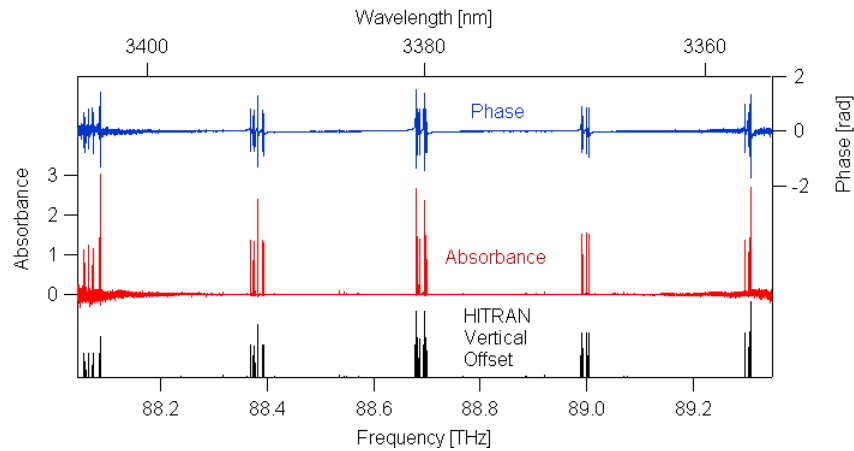


Figure 8: Phase and magnitude measurement of methane lines. The absorbance is also compared to the HITRAN database.

Figure 8 shows the phase and magnitude spectra obtained in the two-branch configuration for a gas cell filled with methane at ~ 200 mTorr. The resolution obtained is 114 MHz, and the covered span is ~ 1.3 THz (corresponding to 10 nm at signal wavelengths around 1550 nm or 50 nm at idler wavelengths around 3400 nm). To improve the SNR, synchronous sampling (and phase compensation) were used to sum successive interferograms [8]. The maximal SNR achieved is 1000 for the phase (i.e., 1 mrad) and 1500 for the magnitude with an integration period of 30 minutes. The number of resolution elements is $1.3 \text{ THz}/114 \text{ MHz} \sim 11,000$ spectral elements, M . The corresponding figure of merit, defined as the product of resolved spectral elements and the average SNR across the spectrum, normalized by the square root of the acquisition period, $SNR_{av.} \times M / \sqrt{t}$, is $\approx 50000\sqrt{\text{Hz}}$. (Note that we normalize by the number of spectral elements, rather than the square root of the number of spectral elements; this normalization is appropriate to an active source where an increased spectral bandwidth will typically reduce the power per spectral bin [17]). For shorter measurement times, the power levels of the 1.5 μm combs and the 1064 nm laser could be further amplified. The center frequency of these initial phase and absorbance measurement of the C-H stretch (ν_3 band P-branch) in methane lies within the 3 – 30 MHz uncertainty of the HITRAN database shown at the bottom of Figure 8.

5. CONCLUSION

We demonstrated DFG combs at $\sim 3.4 \mu\text{m}$ with 200 mHz residual linewidths, a prerequisite to high-precision and high accuracy coherent dual-comb spectroscopy at a wavelength where many fundamental molecular absorption lines are situated. Different interferometric configurations were explored to obtain phase and magnitude spectra of methane. A simpler single-branch setup where only one PPLN and one amplifier for the combs are needed is only appropriate for broad ($> 1\text{GHz}$) spectral features. However, a dual-branch interferometric setup yields higher resolution (limited by the comb repetition rate, here 100 MHz) for phase and magnitude spectra. These initial measurements show good agreement with the HITRAN database. The system has a resolution of 114 MHz, and a frequency accuracy of 1 MHz, and spans 1.3 THz (50 nm at 3.4 μm) in a single measurement. With different filter settings and lock conditions, the 5 THz span of our two combs could be seamlessly covered. Also the resolution of 114 MHz could be doubled by shifting the 1064 nm cw laser by 50 MHz.

Acknowledgements

We thank NTT-electronics for providing the ridge waveguide PPLN. Helpful discussions with Todd Johnson, Kevin Knabe, and Alex Zolot are also acknowledged.

REFERENCES

- [1] Gohle, C., Stein, B., Schliesser, A., Udem, T. and Hänsch, T. W., "Frequency comb vernier spectroscopy for broadband, high-resolution, high-sensitivity absorption and dispersion spectra," *Phys. Rev. Lett.* 99(26), 263902 (2007).
- [2] Giaccari, P., Deschenes, J. D., Saucier, P., Genest, J. and Tremblay, P., "Active fourier-transform spectroscopy combining the direct rf beating of two fiber-based mode-locked lasers with a novel referencing method," *Opt. Express* 16(6), 4347–4365 (2008).
- [3] Johnson, T. A. and Diddams, S. A., "Mid-IR frequency comb upconversion spectroscopy," In *The Conference on Lasers and Electro-Optics (CLEO), CPDB11* (2010).
- [4] Thorpe, M. and Ye, J., "Cavity-enhanced direct frequency comb spectroscopy," *Appl. Phys. B* 91(3), 397–414 (2008).
- [5] Keilmann, F., Gohle, C. and Holzwarth, R., "Time-domain mid-infrared frequency-comb spectrometer," *Opt. Lett.* 29(13), 1542–1544 (2004).
- [6] Schliesser, A., Brehm, M., Keilmann, F. and van der Weide, D., "Frequency-comb infrared spectrometer for rapid, remote chemical sensing," *Opt. Express* 13(22), 9029–9038 (2005).
- [7] Coddington, I., Swann, W. C. and Newbury, N. R., "Coherent multiheterodyne spectroscopy using stabilized optical frequency combs," *Phys. Rev. Lett.* 100(1), 013902 (2008).
- [8] Coddington, I., Swann, W. C. and Newbury, N. R., "Time-domain spectroscopy of molecular free-induction decay in the infrared," *Opt. Lett.* 35, 1395–1397 (2010).
- [9] Bernhardt, B., Ozawa, A., Jacquet, P., Jacquy, M., Kobayashi, Y., Udem, T., Holzwarth, R., Guelachvili, G., Hänsch, T. W. and Picque, N., "Cavity-enhanced dual-comb spectroscopy," *Nature Photon.* 4, 55–57 (2009).
- [10] Erny, C., Moutzouris, K., Biegert, J., Kühlke, D., Adler, F., Leitenstorfer, A. and Keller, U., "Mid-infrared difference-frequency generation of ultrashort pulses tunable between 3.2 and 4.8 μm from a compact fiber source," *Opt. Lett.* 32(9), 1138–1140 (2007).
- [11] Maddaloni, P., Cancio, P. and De Natale, P., "Optical comb generators for laser frequency measurement," *Meas. Sci. Technol.* 20(5), 052001 (2009).
- [12] Takahata, K., Kobayashi, T., Sasada, H., Nakajima, Y., Inaba, H. and Hong, F.-L., "Absolute frequency measurement of sub-doppler molecular lines using a 3.4- μm difference-frequency-generation spectrometer and a fiber-based frequency comb," *Phys. Rev. A* 80(3), 032518 (2009).
- [13] Richter, D., Fried, A. and Weibring, P., "Difference frequency generation laser based spectrometers," *Laser Photonics Rev.* 3 (4), 343–354 (2008).
- [14] Birch, J. R., "Dispersive fourier-transform spectroscopy," *Mikrochim. Acta* 3(1-6), 105–122 (1987).
- [15] Almoayed, N. and Afsar, M., "High-resolution absorption coefficient and refractive index spectra of carbon monoxide gas at millimeter and submillimeter wave-lengths," *IEEE T. Instrum. Meas.* 55(4), 1033–1037 (2006).
- [16] Asobe, M., Tadanaga, O., Yanagawa, T., Umeki, T., Nishida, Y. and Suzuki, H., "High-power mid-infrared wavelength generation using difference frequency generation in damage-resistant Zn : LiNbO₃ waveguide," *Electron. Lett.* 44(4), 288–290 (2008).
- [17] Newbury, N. R., Coddington, I. and Swann, W. C., "Sensitivity of coherent dual-comb spectroscopy," *Opt. Express* 18, 7929–7945 (2010).